



## **A straightforward method for Vacuum-Ultraviolet flux measurements: The case of the hydrogen discharge lamp and implications for solid-phase actinometry**

D. Fulvio, A. C. Brieva, S. H. Cuyllé, H. Linnartz, C. Jäger, and T. Henning

Citation: [Applied Physics Letters](#) **105**, 014105 (2014); doi: 10.1063/1.4887067

View online: <http://dx.doi.org/10.1063/1.4887067>

View Table of Contents: <http://scitation.aip.org/content/aip/journal/apl/105/1?ver=pdfcov>

Published by the [AIP Publishing](#)

---

### **Articles you may be interested in**

[Dynamic photolytical actinometry of the vacuum-ultraviolet radiation produced by multichannel surface discharges of submicrosecond duration](#)

Rev. Sci. Instrum. **78**, 063103 (2007); 10.1063/1.2744225

[Characterization of GaAsP trap detector for radiometric measurements in ultraviolet wavelength region](#)

Rev. Sci. Instrum. **76**, 033110 (2005); 10.1063/1.1866972

[Development of vacuum ultraviolet absorption spectroscopy technique employing nitrogen molecule microdischarge hollow cathode lamp for absolute density measurements of nitrogen atoms in process plasmas](#)

J. Vac. Sci. Technol. A **19**, 599 (2001); 10.1116/1.1340655

[Vacuum ultraviolet absorption spectroscopy employing a microdischarge hollow-cathode lamp for absolute density measurements of hydrogen atoms in reactive plasmas](#)

Appl. Phys. Lett. **75**, 3929 (1999); 10.1063/1.125497

[The breakdown and glow phases during the initiation of discharges for lamps](#)

J. Appl. Phys. **82**, 112 (1997); 10.1063/1.366274

---

The logo for AIP Chaos is centered on a dark red background with a subtle geometric pattern. The letters 'AIP' are in a large, white, sans-serif font, followed by a vertical orange bar and the word 'Chaos' in a smaller, white, sans-serif font.

**AIP | Chaos**

**CALL FOR APPLICANTS**  
Seeking new Editor-in-Chief

## A straightforward method for Vacuum-Ultraviolet flux measurements: The case of the hydrogen discharge lamp and implications for solid-phase actinometry

D. Fulvio,<sup>1,a)</sup> A. C. Brieva,<sup>1</sup> S. H. Cuyllé,<sup>2</sup> H. Linnartz,<sup>2</sup> C. Jäger,<sup>1</sup> and T. Henning<sup>3</sup>

<sup>1</sup>Laboratory Astrophysics Group of the Max Planck Institute for Astronomy at the Friedrich Schiller University Jena, Institute of Solid State Physics, Helmholtzweg 3, D-07743 Jena, Germany

<sup>2</sup>Raymond and Beverly Sackler Laboratory for Astrophysics, Leiden Observatory, Leiden University, P.O. box 9513, 2300 RA Leiden, The Netherlands

<sup>3</sup>Max Planck Institute for Astronomy, Königstuhl 17, D-69117 Heidelberg, Germany

(Received 23 May 2014; accepted 24 June 2014; published online 9 July 2014)

Vacuum-Ultraviolet (VUV) radiation is responsible for the photo-processing of simple and complex molecules in several terrestrial and extraterrestrial environments. In the laboratory such radiation is commonly simulated by inexpensive and easy-to-use microwave-powered hydrogen discharge lamps. However, VUV flux measurements are not trivial and the methods/devices typically used for this purpose, mainly actinometry and calibrated VUV silicon photodiodes, are not very accurate or expensive and lack of general suitability to experimental setups. Here, we present a straightforward method for measuring the VUV photon flux based on the photoelectric effect and using a gold photodetector. This method is easily applicable to most experimental setups, bypasses the major problems of the other methods, and provides reliable flux measurements. As a case study, the method is applied to a microwave-powered hydrogen discharge lamp. In addition, the comparison of these flux measurements to those obtained by O<sub>2</sub> actinometry experiments allow us to estimate the quantum yield (*QY*) values  $QY_{122} = 0.44 \pm 0.16$  and  $QY_{160} = 0.87 \pm 0.30$  for solid-phase O<sub>2</sub> actinometry. © 2014 AIP Publishing LLC. [<http://dx.doi.org/10.1063/1.4887067>]

Vacuum-Ultraviolet (VUV) radiation plays a key role in the photo-processing of gas- and solid-phase molecules in many different terrestrial and extraterrestrial environments, from inter- and circumstellar regions to the atmosphere and the surface of planets, asteroids, and comets.<sup>1–6</sup> For this reason, various chemistry, astronomy, and biology laboratories over the world carry out experimental programs devoted to the study of VUV photoinduced processes on simple and complex molecules.

Lyman- $\alpha$  photons at 122 nm (10.2 eV) constitute a major component of the VUV radiation field in many of these environments,<sup>3,7</sup> explaining why in the last decades there has been a growing interest in simulating the VUV field using microwave-powered hydrogen discharge lamps.<sup>8</sup> The objective of experiments carried out with these lamps is to produce reliable laboratory data allowing the comparison with models and observations. To this purpose, the irradiation source needs to be well characterized in terms of its VUV flux and spectral emission pattern.

Two common ways of carrying out absolute VUV flux measurements are: (1) actinometry and (2) calibrated VUV silicon photodiodes. Actinometry is based on the monitoring of a well characterized chemical reaction as a function of the VUV fluence. A common actinometer for estimating the Lyman- $\alpha$  flux produced by hydrogen discharge lamps is solid-phase O<sub>2</sub>:<sup>9–11</sup> upon VUV photon absorption O<sub>3</sub> is formed from O<sub>2</sub>, a process well documented in the gas-phase.<sup>8</sup> Due to the lack of data for solid-phase O<sub>2</sub> experiments, gas-phase quantum yield (*QY*) values are commonly

used. However, a discrepancy of about a factor of 3 was observed between the flux measurements as determined by solid-phase O<sub>2</sub> actinometry and by a calibrated VUV photodiode.<sup>11</sup> This may be due to the inaccurate assumption that gas-phase *QY* values are suitable for solid-phase experiments. Additional limitations of solid-phase actinometry come from technical requirements. For instance, spectroscopy is typically needed to monitor molecular abundances and a cryostat is required to condense O<sub>2</sub> ( $T \leq 30$  K).

Calibrated VUV photodiodes measure the current induced by VUV irradiation. Although they are considered to be more precise and accurate than actinometry (as their quantum efficiency in the VUV domain is very well documented) their use is much less common. The reason of the prevalent spread of actinometry has to be found in the high cost of calibrated photodiodes and the change in the photocathode surface efficiency (difficult to characterize and monitor) due to atmospheric exposure. In some photodiodes, a passivating oxide layer is used as surface coating in order to protect the photosensitive layer from oxidation and other potential contaminations. However, the passivating layer contributes to the spectral photosensitivity of the diode and is subject to degradation as a result of VUV exposure. The degradation rate depends on the accumulated VUV fluence over time.

In the following, we present an alternative method for VUV flux measurements based on the photoelectric effect. We show how by using this simple method it is possible to obtain reproducible and reliable measurements. As a case study, the method is applied to a microwave-powered hydrogen discharge lamp. In addition, we show how the method

<sup>a)</sup>Electronic addresses: daniele.fulvio@uni-jena.de and dfu@oact.inaf.it

can be applied to estimate the quantum yields for solid-phase actinometry. As an example, we discuss the case for solid-phase  $O_2$ .

Microwave-powered hydrogen discharge lamps consist of a glass tube with a constant flow of  $H_2$  at pressure typically between 0.3 and 1 mbar. The hydrogen is excited by microwave radiation using a McCarroll<sup>12</sup> or Evenson<sup>13</sup> cavity and the microwave generator power is usually kept between 50 and 100 W. The discharge in the lamp is initiated by a Tesla coil. The typical VUV spectrum of hydrogen discharge lamps is dominated by the Lyman- $\alpha$  emission at 122 nm (10.2 eV) and the molecular  $H_2$  emission feature around 160 nm (7.7 eV). The relative ratio between these two features depends on the specific experimental conditions, such as the pressure inside the discharge tube, extra components in the gas flow (for instance, He added to  $H_2$ ), and the relative proportion of these components.<sup>3,14–17</sup> In a typical laboratory setup, the lamp faces the experimental chamber (where the species under study is located) through a VUV-transparent window. The proper choice of the window material is important, as its VUV transmittance can strongly affect the spectrum and photon flux reaching the target. Special care needs to be taken as the VUV radiation can cause degradation of the VUV transmittance of the window over time. For instance, LiF windows, although having high transmittance in the VUV range, degrade significantly within hours of VUV exposure.<sup>11</sup> For experiments with hydrogen discharge lamps,  $MgF_2$  windows are the common choice to guarantee high VUV transmission down to the Lyman- $\alpha$  wavelength while ensuring a high level of resistance against VUV degradation.

The method presented in this Letter to easily determine VUV flux values is based on the photoelectric effect: photoelectrons are emitted from the conduction band of a material once the acquired energy exceeds the work function of the material. Increasing the photon flux increases the number of emitted photoelectrons and the energy of the photoelectrons depends on the energy of the incident photons.

We describe now the experimental procedure, along with a few technical suggestions, before discussing the results. We choose gold as material for the photodetector (the work function of gold is between 4.2 and 5.2 eV, the spread in the value being due to the sensitivity of the work function to the surface contamination status)<sup>18,19</sup> and in practice we use a commercial gold-coated quartz crystal microbalance (QCM)<sup>20,21</sup> as photodetector to carry out the measurements. Although the work function of most metals falls in the 4–5 eV range, gold is a convenient choice as it is inert (therefore does not oxidise in air) and does not degrade upon VUV irradiation. Besides, gold is a material commonly available in laboratory as it is used for a number of purposes (such as IR reflectance standard or coating in QCMs). We propose QCMs because of their small size, compatibility with most systems, and low price.

Figure 1 shows a schematic of the experimental setup and the gold QCM used. The gold photodetector is placed inside an high-vacuum chamber (base  $P < 5 \times 10^{-6}$  mbar) at the sample position, connected by means of a feedthrough to a voltage controlled power supply in a circuit closed by the vacuum chamber itself (grounded). The distance from the source to the detector in our system is about 16 cm. A

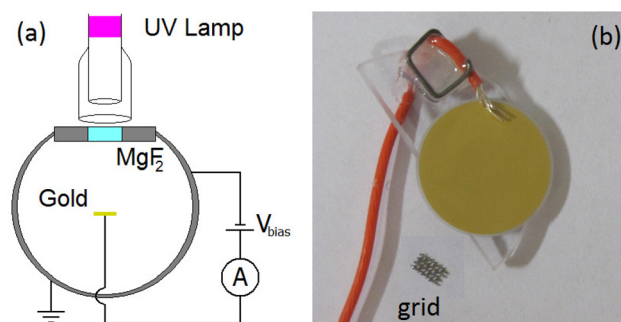


FIG. 1. (a) Schematic of the experimental setup and circuit used in this study. (b) Gold photodetector (diameter = 12.7 mm) mounted on a semicircular support for easy fit at the sample position. The connection detector-circuit is realized by a simple wire touching the gold surface or, when needed, a small metallic grid to facilitate the contact with the gold surface.

microvoltmeter is used to measure the current passing through the circuit. The VUV lamp faces the photodetector through a  $MgF_2$  window as shown in the figure. Unless otherwise specified, the experiments are conducted under constant VUV photon flux and at normal incidence of the VUV light onto the detector. The lamp is always operated with a constant flow of  $H_2$  and a pressure of 0.6 mbar, 100 W are applied by the microwave generator to the Evenson cavity and the reflected power was below 5 W (in most cases equal to 2–3 W) in all experiments.

Ideally, under VUV irradiation, the photoelectrons emitted from the gold surface are collected by the chamber and return to the gold through the circuit represented in Fig. 1. However, there are two additional effects which contribute to the current readings. First, VUV stray light may reach other spots (different than the gold photodetector) inside the chamber, with consequent photoelectron emission, and some of these photoelectrons can be collected by the detector. Second, some of the low energy electrons emitted by the gold detector may return back to it. The “spurious” photoelectrons generated by these two effects contribute antithetically to the current produced by the photoelectrons emitted by the gold surface and collected by the chamber. The contribution of the spurious electrons to the overall current depends on the bias voltage  $V_{bias}$  applied to the gold photodetector, as shown in Fig. 2. When positive or no bias voltage is applied, the spurious photoelectrons counteract the current due to the electrons photoemitted by the gold detector and collected by the chamber. The higher the positive bias voltage applied, the stronger is the electric field which steers the spurious photoelectrons towards the gold surface. Therefore, more of them are collected from increasing distance inside the chamber. On the other hand, when increasing the negative bias voltage applied to the gold surface, the current reaches a maximum value (hereafter referred to as “saturation” current) which remains constant for higher negative values of the potential (Fig. 2). Saturation happens when every photoelectron emitted by the gold is collected by the chamber and, simultaneously, no spurious electrons can reach the gold surface since the electric potential between gold and chamber is greater than their kinetic energy.

The basic concept of our method is that the saturation current is the appropriate parameter to determine the VUV flux at the position of the gold photodetector. If so, the

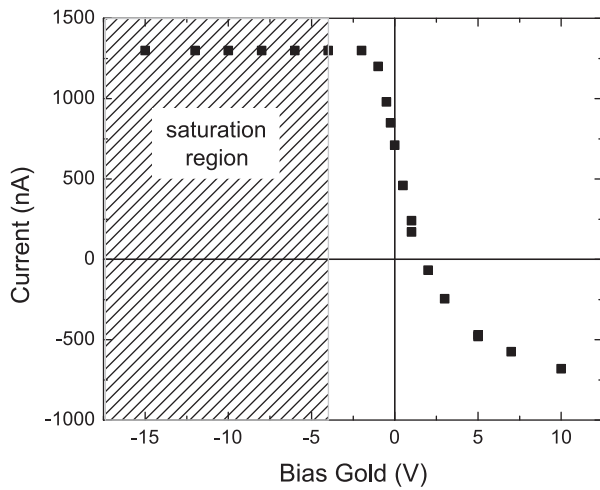


FIG. 2. Total current vs.  $V_{bias}$  applied to the photodetector.

saturation current has to depend linearly on (i) the surface area of the gold detector and (ii) the power applied by the microwave generator, as the VUV flux scales linearly with the surface area and the power applied.<sup>22</sup> We have verified these two points experimentally. Figure 3 presents the results

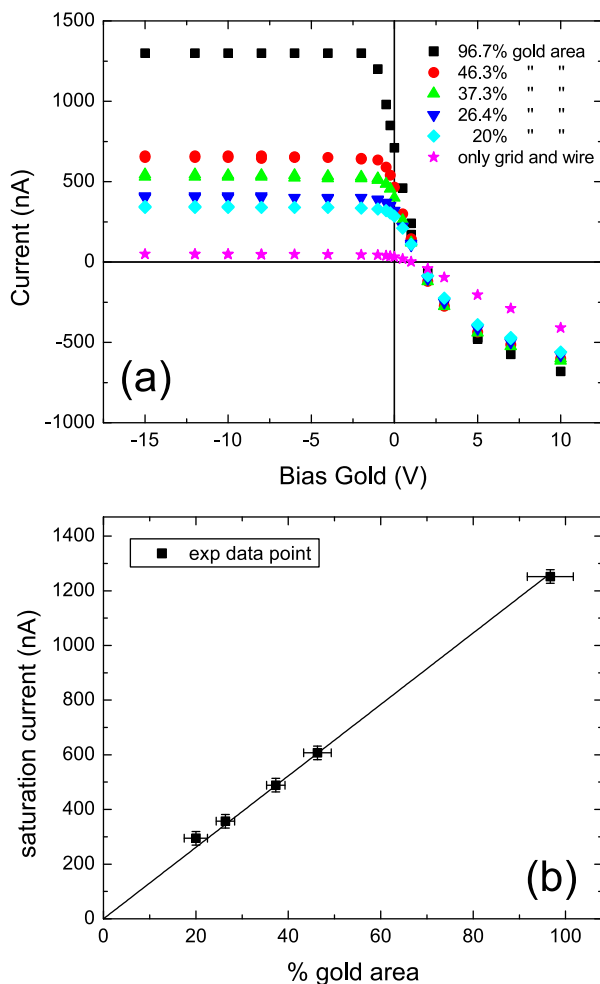


FIG. 3. (a) Same as in Fig. 2 for different surface areas of the gold photodetector. The lowest curve (pink star) shows the current only due to the metallic grid and wire used for the circuit contact with the gold surface. (b) Saturation current for different gold surface areas (from (a)) and best fit to the data points. Saturation current values are plotted after removing the contribution of the grid and wire (pink star curve).

of (i), for the whole range of  $V_{bias}$  (Fig. 3(a)) and the value of the saturation current vs. the surface area of the gold detector (Fig. 3(b)). The area of the photodetector was cut into smaller areas between consecutive experiments. The resulting data points in Fig. 3(b) can be fitted by a straight line passing through the origin as expected for a current which depends only on the flux absorbed. The results of (ii) (not shown for the sake of brevity) confirm the linear correlation between the saturation current and the power applied by the microwave generator in the range of 65–120 W. These two control experiments prove that saturation depends on the VUV flux rather than the limited surface of the gold detector or any other undesirable effect in the circuit.

We now describe the procedure to determine the VUV flux. The total flux  $F_{tot}$  can be divided into the contribution of the spectral components centered at different  $\lambda$ :  $F_{\lambda}$ . Knowing the photoelectric yield  $PY_{\lambda}$  of gold for photons of given wavelength  $\lambda$  and the current  $I_{\lambda}^{sat}$  produced by these photons, the VUV photon flux  $F_{\lambda}$  is

$$F_{\lambda} = \frac{I_{\lambda}^{sat}}{e \times PY_{\lambda} \times A}, \quad (1)$$

where  $e$  is the elementary charge and  $A$  is the irradiated area. VUV spectra of hydrogen discharge lamps are dominated by two spectral features: the Lyman- $\alpha$  emission centered at 122 nm and the molecular  $H_2$  emission around 160 nm. This means that we need to estimate the flux due to each spectral feature:  $F_{122}$  and  $F_{160}$ . To this purpose, two measurements of the saturation current have to be performed: the first one as described above,  $I^{sat1} (= I_{122}^{sat1} + I_{160}^{sat1})$ , and the second one adding an extra window with known transmittance ( $T_{122}$  and  $T_{160}$ ) at the wavelength of each emission feature,  $I^{sat2} (= I_{122}^{sat2} + I_{160}^{sat2})$ . From expression (1), we get a system of two linear equations in two unknowns

$$\begin{cases} I^{sat1} = Ae(PY_{122}F_{122} + PY_{160}F_{160}), \\ I^{sat2} = Ae(PY_{122}T_{122}F_{122} + PY_{160}T_{160}F_{160}). \end{cases} \quad (2)$$

The solution of the system provides the flux for each spectral component. For measuring  $I^{sat2}$ , we use a sapphire window, opaque to the 122-nm component while partially transmitting the 160-nm one. The transmittance  $T_{160}$  of this sapphire window is measured to be 0.5. Solving (2) we find, for the lamp settings discussed before, the following flux values at the detector position (Table I, column 1):  $F_{122} = 1.8 \pm 0.6 \times 10^{14}$  ph  $cm^{-2} s^{-1}$  and  $F_{160} = 3.1 \pm 1.1 \times 10^{14}$  ph  $cm^{-2} s^{-1}$ . We point out that the broadness of the emission band is one of the main error sources, mainly because of the

TABLE I. VUV flux (ph  $cm^{-2} s^{-1}$ ) as measured by the method discussed in this Letter (column 1) and by  $O_2 \rightarrow O_3$  actinometry using the gas-phase value  $QY = 1.92$  (column 2). The last column gives the quantum yield  $QY$  values for solid-phase  $O_2$  actinometry, as estimated from the flux measurements presented in column 1. Values of  $QY$  are in  $O_3$  molecules formed per absorbed photon.

	Flux Gold detector	Flux Actinometry ( $QY = 1.92$ )	Quantum Yield Solid-phase estimate
122 nm	$1.8 \pm 0.6 \times 10^{14}$	$0.4 \pm 0.1 \times 10^{14}$	$QY_{122} = 0.44 \pm 0.16$
160 nm	$3.1 \pm 1.1 \times 10^{14}$	$1.4 \pm 0.35 \times 10^{14}$	$QY_{160} = 0.87 \pm 0.30$

uncertainty on the  $PY_{\lambda}$  value used to estimate the flux from expression (1). We have used  $PY_{122} = 2 \times 10^{-2}$  and  $PY_{160} = 1 \times 10^{-3}$  (in units of photoelectrons per incident photon).<sup>19</sup> We want also to point out that discerning between the two spectral components is required, as recent solid-phase experiments have shown that photoinduced processes can be wavelength dependent.<sup>17,23</sup>

An application of the method discussed in this Letter is the estimation of the quantum yields for solid-phase actinometry. As an example, we discuss the case of solid O<sub>2</sub>. First, we have re-determined the VUV flux by O<sub>2</sub> actinometry experiments (under the same experimental conditions). Inside the high-vacuum chamber, solid O<sub>2</sub> is grown at 11–15 K onto a KBr substrate placed in thermal contact with a closed-cycle helium cryostat. The thickness of the O<sub>2</sub> film is always >1.8 μm (to ensure total absorption of the VUV photons) and is determined by laser interferometry as described in Fulvio *et al.*<sup>24</sup> An FTIR spectrophotometer (Bruker Vertex 80v) is used to record transmittance spectra (resolution: 1 cm<sup>-1</sup>) in the range of 6000–400 cm<sup>-1</sup>. The flux is derived by measuring the area of the ν<sub>3</sub> infrared band of O<sub>3</sub> centered at 1040 cm<sup>-1</sup> as a function of the irradiation time

$$Flux = \frac{Area(\nu_3)}{time \times QY \times A(\nu_3)}, \quad (3)$$

where  $QY$  is the O<sub>3</sub> quantum yield and  $A(\nu_3)$  is the integrated absorption strength for the ν<sub>3</sub> band. While the integrated absorption strength value is known for solid O<sub>3</sub> ( $A(\nu_3) = 1.4 \times 10^{-17}$  cm molecule<sup>-1</sup>),<sup>25</sup> there is a lack of solid-phase data for the O<sub>3</sub> quantum yields. To date, the gas-phase-estimated value  $QY = 1.92$  has been commonly used. Employing  $QY = 1.92$ , we find the flux values reported in column 2 of Table I. These values are about a factor of 3 smaller than the flux values obtained using the gold photodetector (column 1). This trend is similar to the one found when comparing the flux measurements obtained by solid-phase O<sub>2</sub> actinometry and a calibrated VUV photodiode.<sup>11</sup> We think that the discrepancy may be due to the use of gas-phase  $QY$  values for solid-phase experiments. Knowing the flux values from the measurements with the gold photodetector and using expression (3), we estimate the  $QY$  values for solid-phase O<sub>2</sub> actinometry as reported in column 3. However, the precision of these estimates strongly depends on the precision on the measurements of the photoelectric yields of gold. In this view, our results suggest the need for more precise photoelectric yield measurements.

Finally, we want to point out two additional advantages of our method for VUV flux measurements: (1) the response of the photodetector is “limited” to 5–11 eV; this is the spectral range where the lamp emission simultaneously induces photoelectric effect on gold and is transmitted by the MgF<sub>2</sub> window; on the other hand, the spectral response of VUV silicon photodiodes extends to the visible and IR range; this last case may lead, if neglected, to an overestimated VUV flux measurement; (2) our method can be used even in conditions of “rough” vacuum: when slowly increasing the pressure in the vacuum chamber, our measurements remain unaffected up to  $1 \times 10^{-2}$  mbar; this is another advantage with respect to actinometry.

In summary, we present a straightforward method to determine the VUV flux and discuss in detail the case of a commonly used microwave-powered hydrogen discharge lamp. Technical details and pragmatic suggestions are provided. The main advantages of the proposed method and detector can be summarized as follows: no need for spectroscopy; no need for cryogenic components; response in the spectral region 5–11 eV, low cost, small size and easy fitting in almost every system; suitable for chamber pressure up to  $1 \times 10^{-2}$  mbar. Finally, the method here presented can be applied to estimate the quantum yields for solid-phase actinometry. As an example, the case of solid-phase O<sub>2</sub> actinometry has been discussed.

This research has received funding from the European Community’s Seventh Framework Programme (FP7/2007-2013) under Grant Agreement No. 238258. A.C.B. acknowledges support by the EU FP7-Marie-Curie IEF (Grant Agreement No. 274794).

<sup>1</sup>P. Weber and J. M. Greenberg, *Nature* **316**, 403 (1985).

<sup>2</sup>P. A. Gerakines, W. A. Schutte, and P. Ehrenfreund, *Astron. Astrophys.* **312**, 289 (1996).

<sup>3</sup>H. Cottin, P. Coll, D. Coscia, N. Fray, Y. Y. Guan, F. Macari, F. Raulin, C. Rivron, F. Stalport, C. Szopa, D. Chaput, M. Viso, M. Bertrand, A. Chabin, L. Thirkell, F. Westall, and A. Brack, *Adv. Space Res.* **42**, 2019 (2008).

<sup>4</sup>M. E. Palumbo, G. A. Baratta, D. Fulvio, M. Garozzo, O. Gomis, G. Leto, F. Spinella, and G. Strazzulla, *J. Phys. Conf. Ser.* **101**, 012002 (2008).

<sup>5</sup>K. I. Öberg, E. F. van Dishoeck, and H. Linnartz, *Astron. Astrophys.* **496**, 281 (2009).

<sup>6</sup>D. Fulvio, U. Raut, and R. A. Baragiola, *Astrophys. J., Lett.* **752**, L33 (2012).

<sup>7</sup>J. S. Mathis, P. G. Mezger, and N. Panagia, *Astron. Astrophys.* **128**, 212 (1983).

<sup>8</sup>P. Warneck, *Appl. Opt.* **1**, 721 (1962).

<sup>9</sup>P. A. Gerakines, M. H. Moore, and R. L. Hudson, *Astron. Astrophys.* **357**, 793 (2000).

<sup>10</sup>G. A. Baratta, G. Leto, and M. E. Palumbo, *Astron. Astrophys.* **384**, 343 (2002).

<sup>11</sup>H. Cottin, M. H. Moore, and Y. Bénilan, *Astrophys. J.* **590**, 874 (2003).

<sup>12</sup>B. McCarroll, *Rev. Sci. Instrum.* **41**, 279 (1970).

<sup>13</sup>F. C. Fehsenfeld, K. M. Evenson, and H. P. Broida, *Rev. Sci. Instrum.* **36**, 294 (1965).

<sup>14</sup>P. Jenniskens, G. A. Baratta, A. Kouchi, M. S. de Groot, J. M. Greenberg, and G. Strazzulla, *Astron. Astrophys.* **273**, 583 (1993).

<sup>15</sup>M. S. Westley, R. A. Baragiola, R. E. Johnson, and G. A. Baratta, *Planet. Space Sci.* **43**, 1311 (1995).

<sup>16</sup>G. M. Muñoz Caro and W. A. Schutte, *Astron. Astrophys.* **412**, 121 (2003).

<sup>17</sup>Y.-J. Chen, K.-J. Chuang, G. M. Muñoz Caro, M. Nuevo, C.-C. Chu, T.-S. Yih, W.-H. Ip, and C.-Y. R. Wu, *Astrophys. J.* **781**, 15 (2014).

<sup>18</sup>D. E. Eastman, *Phys. Rev. B* **2**, 1 (1970).

<sup>19</sup>B. Feuerbacher and B. Fitton, *J. Appl. Phys.* **43**, 1563 (1972).

<sup>20</sup>M. A. Allodi, R. A. Baragiola, G. A. Baratta, M. A. Barucci, G. A. Blake, P. Boduch, J. R. Brucato, C. Contreras, S. H. Cuyllé, D. Fulvio, M. S. Gudipati, S. Ioppolo, Z. Kanuchova, A. Lignell, H. Linnartz, M. E. Palumbo, U. Raut, H. Rothard, F. Salama, E. V. Savchenko, E. Sciamma-O’Brien, and G. Strazzulla, *Space Sci. Rev.* **180**, 101 (2013).

<sup>21</sup>Also known as “un-polished” or “diffuse” gold QCMs.

<sup>22</sup>Y. Bénilan, M.-C. Gazeau, E.-T. Es-Sebbar, A. Jolly, E. Arzoumanian, N. Fray, and H. Cottin, in *EPSC-DPS Joint Meeting* (2011), p. 1317.

<sup>23</sup>E. C. Fayolle, M. Bertin, C. Romanzin, X. Michaut, K. I. Öberg, H. Linnartz, and J.-H. Fillion, *Astrophys. J., Lett.* **739**, L36 (2011).

<sup>24</sup>D. Fulvio, B. Sivaraman, G. A. Baratta, M. E. Palumbo, and N. J. Mason, *Spectrochim. Acta, Part A* **72**, 1007 (2009).

<sup>25</sup>B. D. Teolis, M. Famá, and R. A. Baragiola, *J. Chem. Phys.* **127**, 074507 (2007).